Analytical and Bioanalytical Chemistry (2019) 411:639–646
https://doi.org/10.1007/s00216-018-1365-3

RESEARCH PAPER

MMP-11 as a biomarker for metastatic breast cancer by immunohistochemical-assisted imaging mass spectrometry

Raquel González de Vega[1,2] · David Clases[2] · María Luisa Fernández-Sánchez[1] · Noemí Eiró[3] · Luis O. González[3,4] · Francisco J. Vizoso[3] · Philip A. Doble[2] · Alfredo Sanz-Medel[1]

Received: 12 July 2018 / Revised: 20 August 2018 / Accepted: 6 September 2018 / Published online: 15 September 2018

Abstract

MMP-11 is a member of the matrix metalloproteinase family (MMPs) which are overexpressed in cancer cells, stromal cells and the adjacent microenvironment. The MMP protein family encompasses zinc-dependent endopeptidases that degrade the extracellular matrix (ECM), facilitating the breakdown of the basal membrane and matrix connective tissues. This function is believed to be important in cancer development and metastasis. This paper investigated a gold nanoparticle-based immunohistochemical assay to visualise the distribution of MMP-11 in human breast cancer tissues from eight patients with and without metastases by employing laser ablation inductively coupled plasma mass spectrometry (LA-ICP-MS). The expression of MMP-11 was increased and more heterogeneous in metastatic specimens compared to non-metastatic tumour samples. These findings demonstrate that imaging breast tumours by LA-ICP-MS may be a useful tool to aid the prognosis and treatment of breast cancer. As an example, samples of two patients are presented who were diagnosed with matching characteristics and grades of breast cancer. Although both patients had a similar prognosis and treatment, only one developed metastases.

Keywords Laser ablation · Biological samples · Immunoassays/ELISA · Mass spectrometry/ICP-MS

Introduction

Matrix metalloproteinases (MMPs) belong to a large family of zinc-dependent endopeptidases that contribute to tissue remodelling by degrading the extracellular matrix (ECM). MMPs are characterised by their structure and substrate specificity into several groups: collagenases, gelatinases, stromelysins, matrilysins and membrane-type MMPs [1]. MMP-11 was discovered in 1990 from a gene overexpression in a cDNA library for human breast cancer biopsies [2]. This proteolytic enzyme, through degradation of ECM, may promote tumour growth and invasion, angiogenesis, recruitment of inflammatory cells and metastases [3]. Clinical trials have demonstrated that an overexpression of MMP-11 is correlated with reduced survival rates among patients with breast, head, neck or colon cancer [4]. It was therefore concluded that MMP-11 plays a key role in the progression of cancer. However, the overexpression of MMP-11 also offers potential as a biomarker for an early diagnosis, prognosis and adapted treatments [5]. Roscilli et al. studied the overexpression of MMP-11 in breast and prostate cancers and confirmed that

Published in the topical collection *Elemental and Molecular Imaging by LA-ICP-MS* with guest editor Beatriz Fernández García.

Electronic supplementary material The online version of this article (https://doi.org/10.1007/s00216-018-1365-3) contains supplementary material, which is available to authorized users.

✉ María Luisa Fernández-Sánchez
marisafs@uniovi.es

✉ Philip A. Doble
Philip.Doble@uts.edu.au

[1] Department of Physical and Analytical Chemistry, Faculty of Chemistry, University of Oviedo, C/Julio Claveria 8, 33006 Oviedo, Spain

[2] Elemental Bio-imaging Facility, University of Technology Sydney, Sydney, New South Wales 2007, Australia

[3] Research Unit, Hospital de Jove Foundation, Avda. Eduardo Castro 161, 33290 Gijón, Spain

[4] Department of Anatomical Pathology, Hospital de Jove Foundation, Avda. Eduardo Castro 161, 33290 Gijón, Spain

MMP-11 is a promising biomarker and a suitable target for cancer immunotherapeutic strategies [6].

MMP-11 is involved in both normal and pathological remodelling processes and is predominantly expressed by fibroblasts and mononuclear inflammatory cells [7, 8]. A recent study by Eiro et al. [9] demonstrated the expression of MMP-11 by mononuclear inflammatory cells (MICs) and suggested that it is a potent prognostic factor which may be exploited to predict the course of an associated cancer in terms of malignancy. MMP-11 has multiple functions in several types of cells and tissues in the tumour microenvironment which may exert its influence upon cancer pathogenesis. Therefore, the differential expression of MMP-11 and its distribution pattern within the heterogeneous environment of cancer and healthy tissue may provide novel insights for diagnosis, classification and prognosis. In this context, the combination of epidemiological, analytical and biological studies becomes increasingly relevant for the investigation of MMP-11 and its role in breast cancer.

Elemental bio-imaging (EBI) by inductively coupled plasma mass spectrometry (LA-ICP-MS) is gaining increasing importance for the investigation of the metallome [10]. The combination of LA-ICP-MS and immunohistochemistry (IHC) involves labelling antibodies with metal tags to image target biomolecules [11, 12]. Various IHC protocols are readily available and allow the labelling of multiple proteins or other biomolecules with distinct metals that are spatially resolvable by LA-ICP-MS. The potential of IHC-assisted LA-ICP-MS for a multiplexed analysis of antigens has already been demonstrated in several studies [13, 14]. This has particular applicability for cancer pathogenesis since biomarkers may be imaged with high sensitivity and high spatial (cellular) resolution [15–17]. Calibration for robust relative quantification of biomarkers is highly desirable as it allows reliable comparison of expression levels among numerous samples [18]. IHC-assisted LA-ICP-MS may also be incorporated into clinical practice with multiplexed analysis of microarrays for high sample throughput and the determination of several biomarkers simultaneously [13, 17].

In this work, a gold nanoparticle-based immunoassay was developed for measuring MMP-11 expression and mapping its distribution pattern in breast cancer tissues. As MMP-11 is involved in breast cancer initiation, progress and metastases development, breast cancer samples with and without metastases were selected, sampled, analysed and compared. A two-step immunoassay was developed where an anti-MMP-11 primary antibody was first incubated on breast cancer tissue and subsequently labelled with a metal-tagged secondary antibody to visualise by ICP-MS the MMP-11 expression and distribution in normal and cancerous areas of the biological specimens.

Experimental

Sample collection

Eight breast cancer samples were obtained from patients with histologically confirmed diagnosis of early invasive breast cancers of ductal types (see Table 1). Four of the eight patients developed metastases. Paraffin-embedded human breast cancer samples were obtained from the Hospital de Jove Foundation (Gijon, Spain). The study adheres to national regulations and was approved by the Hospital de Jove Foundation Ethics and Investigation Committee (PI02/2018). H&E-stained tissue sections of areas of interest of all cancer samples were provided to locate and characterise the tumour and stroma within the tissue.

Tissue staining procedure

Tissue sections were dewaxed using xylene (Merk Millipore, Darmstadt, Germany) and aqueous solutions made of decreasing amounts of ethanol (Merk Millipore). The samples were then washed in Milli Q water (18.2 MΩ; Merk Millipore) and equilibrated in phosphate-buffered saline (PBS, Sigma Aldrich, St Louis, MO, USA) for 10 min. A blocking solution was applied to the tissue sections for 5 min at room temperature with peroxidase-blocking reagent (3% H_2O_2) to avoid non-specific staining. The diluted (1:1000) primary antibody (anti-MMP-11 mouse monoclonal antibody, Thermo Fisher, Massachusetts, USA) was then incubated onto the sections for 1 h. The sections were then rinsed with tris-buffered saline (TBS 1× and 0.05% Tween 20 (TBST)) to remove unbound antibodies. Finally, the sections were incubated in a diluted (1:100) gold (5-nm particle size)-labelled secondary antibody

Table 1 Clinicopathological characteristics of the eight patients with invasive breast ductal carcinoma. Tumour size: T1 > 2 cm, T2 2–5 cm and T3 > 5 cm; Stage: based on tumour size, metastases and affection to lymph nodes. Histological grade (SBR): well, moderate and poorly differentiate (1, 2 and 3, respectively). Samples 1–4 are non-metastatic and 5–8 developed metastases

Sample	Tumour size (T)	Stage of the tumour	Lymph nodes affected	Histological grade (SBR)	Oestrogen receptor (ER)
1	2	2	No	2	+
2	2	2	No	2	+
3	1	2	Yes	1	–
4	1	2	Yes	3	+
5	1	2	Yes	2	–
6	1	1	No	3	+
7	2	2	No	3	–
8	1	2	Yes	3	+

solution (Anti-mouse IgG, Sigma Aldrich) for 30 min and washed with TBST.

For comparisons and validation, a colorimetric IHC standard staining of MMP-11 was performed in consecutive breast tissue section following the protocol described by Vizoso et al. [19] to verify the efficiency of the above described gold immunoassay.

Instrumentation

LA-ICP-MS experiments were performed with a CETAC LSX-213 G2+ laser ablation system (Teledyne CETAC Technologies, Omaha, NE, USA) equipped with an aerosol rapid introduction system (ARIS, Teledyne CETAC) and coupled to a Thermo iCAP RQ ICP-MS (Thermo Fisher). Helium was used as the carrier gas (99.999% purity, BOC, North Ryde, NSW, Australia). The LA-ICP-MS system was tuned for maximum sensitivity prior to each experiment using the reference material NIST 612 "Trace Elements in Glass". The ICP-MS was operated in standard mode and also tuned to minimise the formation of oxides by monitoring the oxide ratio ($^{232}Th^{16}O^{+}/^{232}Th^{+}$, m/z 248/232 < 1%). Furthermore, the isotope ratios were monitored to confirm the absence of interfering polyatomic species. Typical instrumental parameters are summarised in Table 2. Images were analysed and created with the imaging software MassImager 3.31 by Robin Schmid (University of Muenster, Germany).

Calibration strategy

External calibration using matrix-matched gelatine standards was used for the quantification of Zn and Au. Calibration curves were constructed by plotting the signal intensity of $^{66}Zn^{+}$ and $^{197}Au^{+}$ obtained by LA-ICP-MS vs. the standards concentration (1, 5, 10, 15 and 25 ppm for Zn and 0.1, 0.25, 0.5, 0.75 and 1 ppm for Au). The correlation coefficients of calibration curves were 0.9933 and 0.9912 for $^{66}Zn^{+}$ and $^{197}Au^{+}$, respectively. Using the obtained linear regressions, each data point (voxel) recorded by LA-ICP-MS was converted into concentrations. The exact Zn and Au levels of the different gelatine standards were determined in triplicate by solution nebulisation ICP-MS.

Table 2 Operating conditions for the ICP-MS and laser ablation system

Thermo ICAP RQ	
RF power	1550 W
Ar make-up gas	0.9 L min^{-1}
Isotopes	Mn^{55}, Fe^{57}, Cu^{63}, ^{66}Zn and ^{197}Au
Integration times	0.05 s
CETAC LSX-213 G2+	
Laser wavelength	213 nm
Pulse energy	20% (1.64 J/cm^2)
Repetition rate	20 Hz
Spot size	30 μm
Scan speed	120 μm s^{-1}
Carrier gas flow rate	0.4 L min^{-1} He

Results and discussion

Figure 1 shows the Au distribution representing the expression of MMP-11 across two exemplar samples of non-metastatic and metastatic tumours. Sample 1a had no evidence of metastasis, whereas sample 1b was identified as metastatic. Various regions of interest consisting of tumour only, tumour and stroma and stroma only were identified by a pathologist via H&E-stained consecutive tissue sections and were compared against the MMP-11 distribution. In general, the non-metastatic sample 1a when compared again the metastatic sample 1b had relatively homogeneous distributions of MMP-11, even across tumorous areas.

Figure 1a contained six regions of interest. Three of these regions in Fig. 1a, regions 1, 2 and 3 contained the tumour and showed elevated relative MMP-11 levels, with average Au values of approximately 300 ng/g. These distributions confirm that the growth of the tumour was connected to breakdown of the surrounding tissue, which requires the expression of distinct proteases such as MMP-11. The metastatic sample (Fig. 1b) contained several individual tumours across the tissue. The stroma and the tumour regions contained significantly increased levels of MMP-11 in comparison to the non-metastatic tumour, which was likely associated with its increased growth and spread. Due to the metastases, MMP-11 was more heterogeneously distributed throughout the tissue with several hotspots exceeding concentrations of 600 ng/g of Au. Further comparison between the H&E sections and MMP-11 distribution of the eight samples involved in this study are provided as Electronic Supplementary Material (ESM Figs. S1–S8), showing that the increase in MMP-11 heterogeneity and expression was consistent across all metastatic samples compared with the non-metastatic tumours.

The spatial distribution of MMP-11 from two patients with similar cancer characteristics is shown in Fig. 2. Both patients (corresponding to sample 4 and 8 in Table 1) were graded with matching tumour sizes, stages and histological status. Both cancers affected the lymph nodes and the oestrogen receptor (ER) was graded as positive. As such, both patients had a similar prognosis and treatment regimens. However, the course of the disease developed differently and only one of the patients developed metastases. As before, the non-metastatic sample had a more uniform distribution, whilst the metastatic sample had elevated MMP-11 levels with

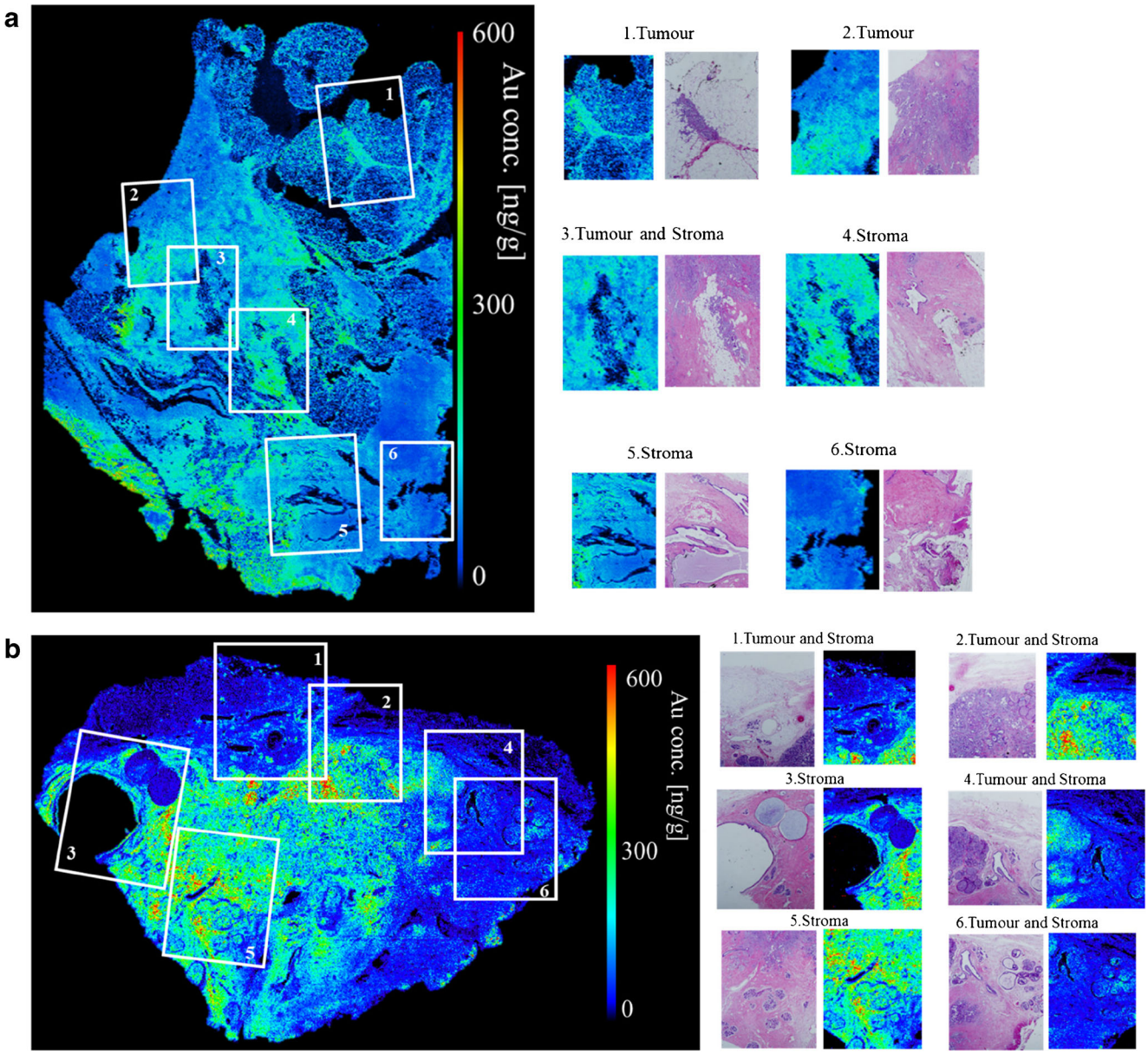

Fig. 1 MMP-11 distribution in two cancer tissue sections. **a** A non-metastatic and **b** a metastatic samples. The samples correspond to the samples 3 and 6 in Table 1, respectively

several hot spots. A comparison with the H&E-stained tissue sections revealed a co-localisation of cancer and metastases with the MMP-11 enzyme across the tissue. The increased breakdown of the surrounding tissue caused by MMP-11 is consistent with the hypothesis that MMP-11 is involved in both the mitosis and metastases of the tumour and that MMP-11 is a viable biomarker for malignancy.

Zn is known to be integral to MMP-11 and was previously investigated by de Vega et al. in a comparative study using LA-ICP-MS and MALDI-IMS, which revealed a correlation of the Zn distribution with the MMP-11 localisation [20]. Therefore, the Zn and MMP-11 (Au) distribution of two samples (without (a) and with metastasis (b) (samples 1 and 7, respectively)) is compared in Fig. 3. Here, the metastatic sample showed the expected increase of heterogeneity and elevated MMP-11 levels exceeding 600 ng/g compared to the non-metastatic sample. However, a correlation between Zn and MMP-11 was not found. This apparent contradiction to the previous findings by de Vega et al. may be explained by Zn losses during the paraffination, deparaffinisation and washing steps during the staining process [21, 22]. Fresh-cut frozen sections are required to investigate this apparent anomaly.

A colorimetric IHC standard staining method was applied to visualise and validate the expression of MMP-11 in consecutive breast tissue sections. Figure 4 compares data

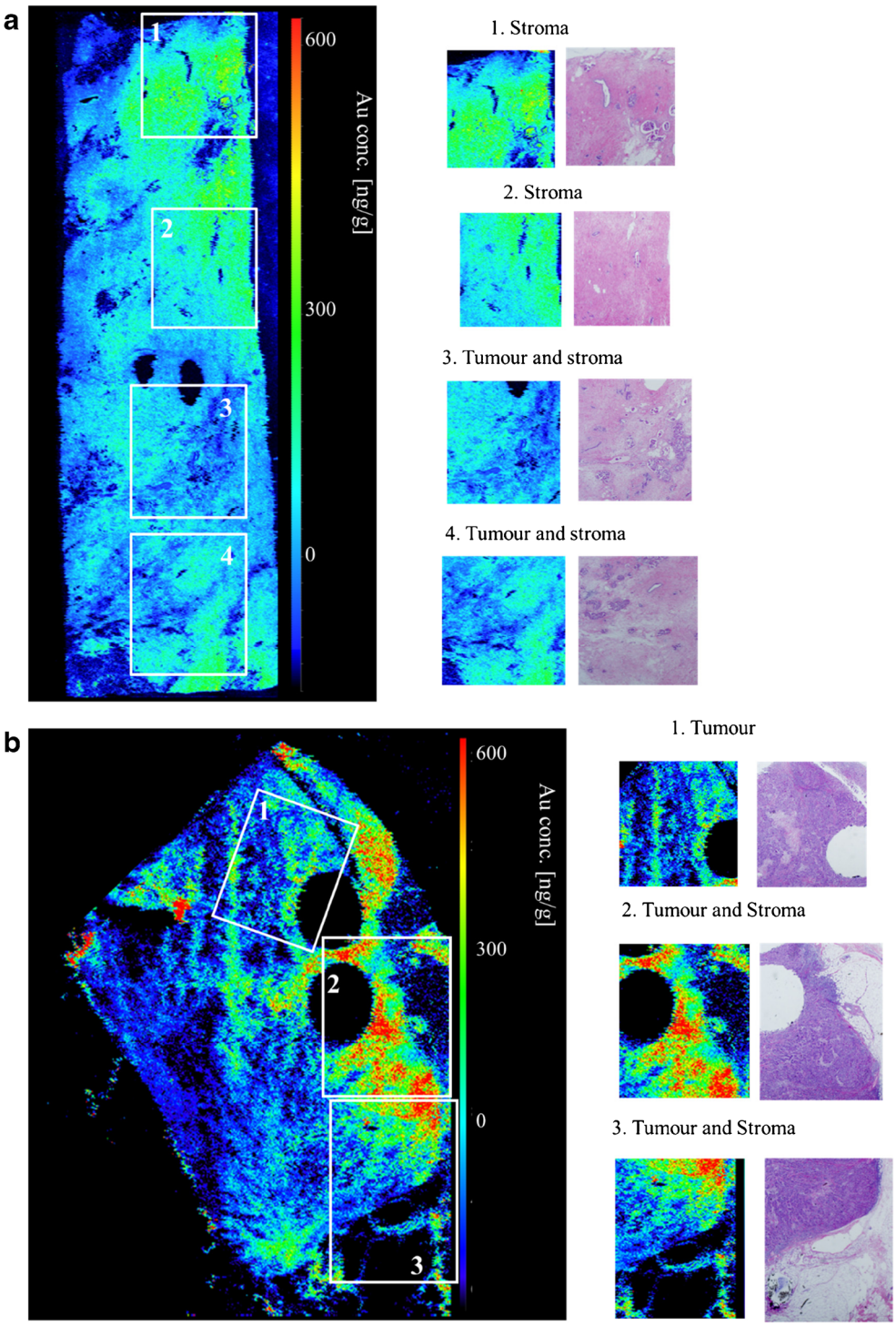

Fig. 2 $^{197}Au^{+}$ distribution obtained by LA-ICP-MS of two breast cancer tissue samples, without ((**a**) sample 4) and with metastasis ((**b**) sample 8) after the IHC staining

obtained by IHC-assisted LA-ICP-MS, H&E stainings and standard IHC colorimetric stainings of three representative samples (samples 3, 6 and 7, respectively). The hotspots visible by H&E and common IHC colour staining are in line with the results obtained via IHC-assisted LA-ICP-MS. However, it is apparent that the latter has a higher degree of contrast whilst also allowing more objective, quantitative interpretations.

Conclusions

IHC-assisted LA-ICP-MS was applied to the quantitative expression and mapping of the cancer biomarker MMP-11 in human breast cancer tissue sections. The analysis of pre-labelled antibodies resulted in an increased sensitivity due to the fact that several Au atoms are linked as a nanoparticle to each antibody, respectively.

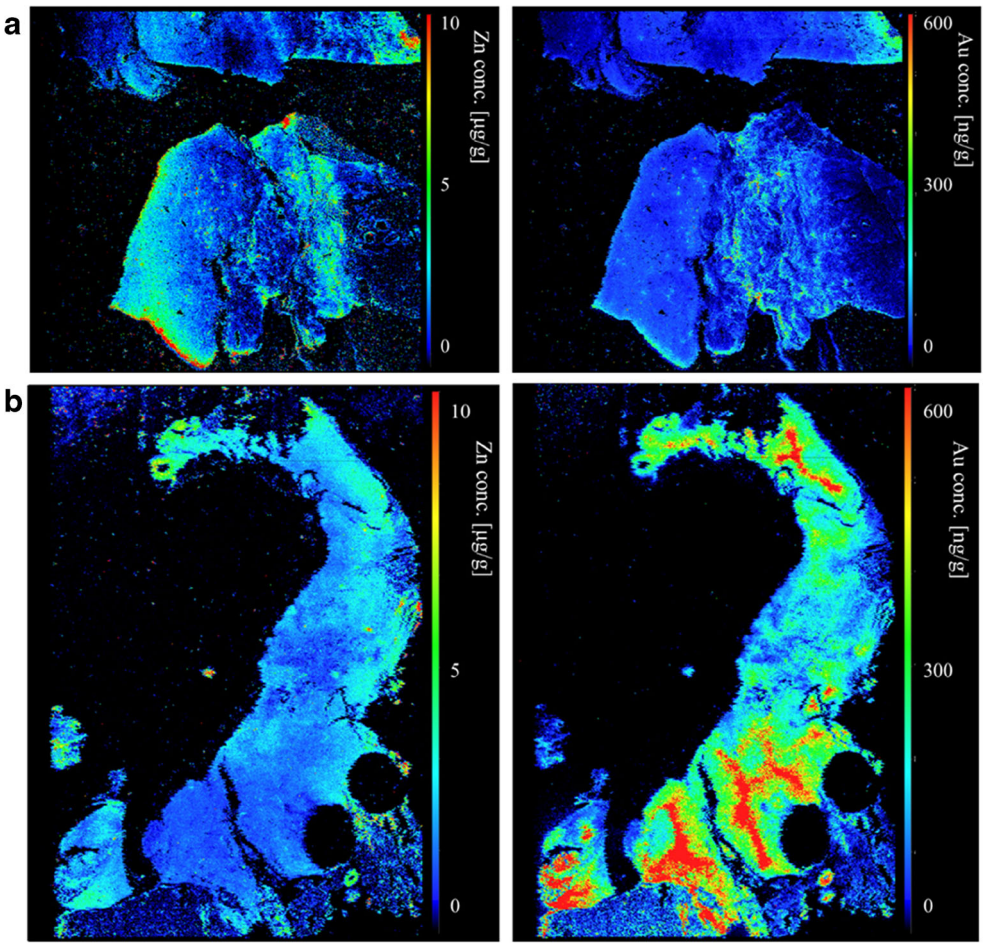

Fig. 3 Elemental distribution obtained by LA-ICP-MS showing the Au/MMP-11 and Zn distribution of two breast cancer tissue samples, without (**a**) and with metastasis (**b**) (samples 1 and 7, respectively (Table 1))

Whilst the presence of MMP-11 was detected in both metastatic and non-metastatic samples, metastatic samples contained a more heterogeneous distribution with several accumulations highly localised within the cancerous tissue. Higher MMP-11 levels (exceeding 600 ng/g Au) were found in the stroma and tumours of the metastatic sample which was linked to an increased growth rate of the tumour presumed to be facilitated by increased breakdown of the surrounding tissue by proteases such as MMP-11. The non-metastatic sample contained lower MMP-11 levels with average levels of 300 ng/g (expressed as Au). The case of two patients, who shared the same cancer grading and an identical prognosis was

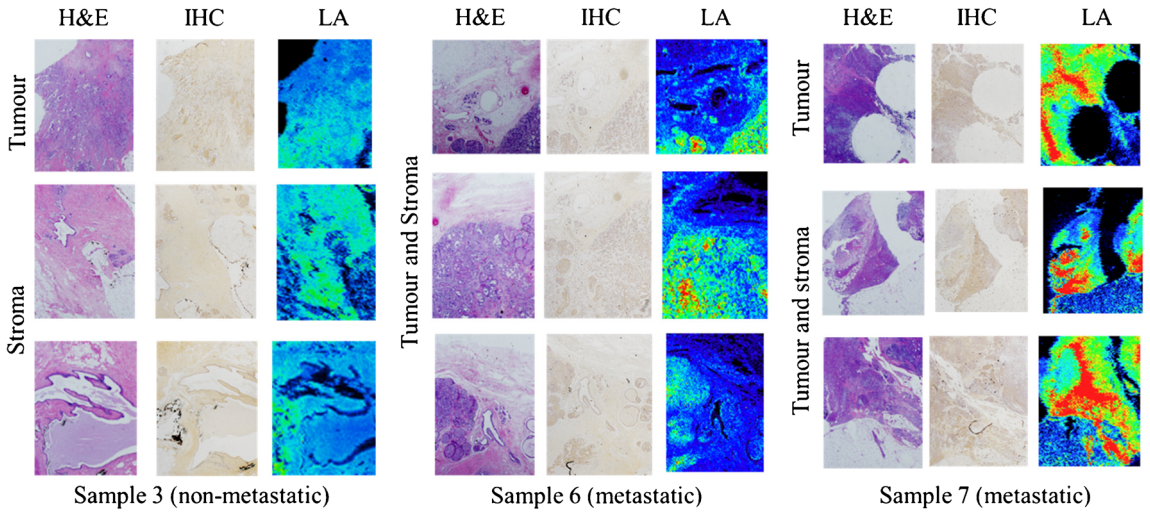

Fig. 4 Comparative images obtained from three tumour tissues by LA-ICP-MS (Au distribution) and IHC (MMP-11) (sample 3, 6 and 7, respectively)

discussed. Despite the similarities, an identical prognosis and treatment one patient developed metastases whilst the cancer of the other patient did not spread. This investigation via IHC-assisted LA-ICP-MS has proved to be promising to reveal differences in the expression and homogeneity of MMP-11 in both metastatic and non-metastatic cancer, demonstrating that MMP-11 may be a viable and sensitive biomarker for prognostic determinations of breast cancer metastases. Future work involves the determination of threshold values and to investigate the potential to integrate the determination of MMP-11 into clinical practice to improve breast cancer characterisation, prognoses and treatment.

Funding information This work was support by projects MINECO-17-CTQ2016-79412-P from the Spanish Government co-financed by FEDER programme of the European Union (EU), FC-15-GRUPIN14-092 from Fundación para la Investigación Científica Aplicada y la Tecnología (FICYT) from Principado de Asturias co-financed by EU and PAD is the recipient of an Australian Research Council Discovery Project (DP170100036).

Compliance with ethical standards

The study adheres to national regulations and was approved by the Hospital de Jove Foundation Ethics and Investigation Committee (PI02/2018). All procedures performed in studies involving human participants were in accordance with the ethical standards of the institutional and/or national research committee and with the 1964 Helsinki declaration and its later amendments or comparable ethical standards. Informed consent was obtained from all individual participants included in the study.

Conflict of interest The authors declare that they have no conflict of interests.

References

1. Pulido-Olmo H, Rodríguez-Sánchez E, Navarro-García JA, Barderas MG, Álvarez-Llamas G, Segura J, et al. Rapid, automated, and specific immunoassay to directly measure matrix metalloproteinase-9-tissue inhibitor of metalloproteinase-1 interactions in human plasma using AlphaLISA technology: a new alternative to classical ELISA. Front Immunol. 2017;8:1–12. https://doi.org/10.3389/fimmu.2017.00853.
2. Basset P, Bellocq J, Wolf C, Stoll P, Hutin P, Limacher J, et al. A novel metallopreoteinase gene specifically expressed in stromal cells of breast cancer. Nature. 1990;348:699–704.
3. Bremnes RM, Dønnem T, Al-Saad S, Al-Shibli K, Andersen S, Sirera R, et al. The role of tumor stroma in cancer progression and prognosis: emphasis on carcinoma-associated fibroblasts and non-small cell lung cancer. J Thorac Oncol. 2011;6:209–17. https://doi.org/10.1097/JTO.0b013e3181f8a1bd.
4. Naghshvar F, Torabizadeh Z, Charati JY, Akbarnezhad M. Relationship between MMP-11 expression in invasive ductal breast carcinoma with its clinicopathologic parameters. Middle East J Cancer. 2017;8:69–75.
5. Zhang X, Huang S, Guo J, Zhou L, You L, Zhang T, et al. Insights into the distinct roles of MMP-11 in tumor biology and future therapeutics (review). Int J Oncol. 2016;48:1783–93. https://doi.org/10.3892/ijo.2016.3400.
6. Roscilli G, Cappelletti M, De Vitis C, Ciliberto G, Di Napoli A, Ruco L, et al. Circulating MMP11 and specific antibody immune response in breast and prostate cancer patients. J Transl Med. 2014;12:54. https://doi.org/10.1186/1479-5876-12-54.
7. Eiro N, González L, Martínez-Ordoñez A, Fernandez-Garcia B, González LO, Cid S, et al. Cancer-associated fibroblasts affect breast cancer cell gene expression, invasion and angiogenesis. Cell Oncol. 2018;41:369–78. https://doi.org/10.1007/s13402-018-0371-y.
8. González L, Eiro N, Fernandez-Garcia B, González LO, Dominguez F, Vizoso FJ. Gene expression profile of normal and cancer-associated fibroblasts according to intratumoral inflammatory cells phenotype from breast cancer tissue. Mol Carcinog. 2016;55:1489–502. https://doi.org/10.1002/mc.22403.
9. Eiró N, Fernandez-Garcia B, Vázquez J, Delcasar JM, González LO, Vizoso FJ. A phenotype from tumor stroma based on the expression of metalloproteases and their inhibitors, associated with prognosis in breast cancer. Oncoimmunology. 2015;4:1–11. https://doi.org/10.4161/2162402X.2014.992222.
10. Konz I, Fernández B, Fernández ML, Pereiro R, Sanz-Medel A. Laser ablation ICP-MS for quantitative biomedical applications. Anal Bioanal Chem. 2012;403:2113–25. https://doi.org/10.1007/s00216-012-6023-6.
11. Zhang C, Wu F, Zhang Y, Wang X, Zhang X. A novel combination of immunoreaction and ICP-MS as a hyphenated technique for the determination of thyroid-stimulating hormone (TSH) in human serum. J Anal At Spectrom. 2001;16:1393–6. https://doi.org/10.1039/B106387C.
12. Baranov V, Quinn Z, Bandura D, Tanner S. A sensitive and quantitative element-tagged immunoassay with ICPMS detection. Anal Chem. 2002;74:1629–36.
13. Seuma J, Bunch J, Cox A, McLeod C, Bell J, Murray C. Combination of immunohistochemistry and laser ablation ICP mass spectrometry for imaging of cancer biomarkers. Proteomics. 2008;8:3775–84. https://doi.org/10.1002/pmic.200800167.
14. Roos PH, Venkatachalam A, Manz A, Waentig L, Koehler CU, Jakubowski N. Detection of electrophoretically separated cytochromes P450 by element-labelled monoclonal antibodies via laser ablation inductively coupled plasma mass spectrometry. Anal Bioanal Chem. 2008;392:1135–47. https://doi.org/10.1007/s00216-008-2242-2.
15. Giesen C, Mairinger T, Khoury L, Waentig L, Jakubowski N, Panne U. Multiplexed immunohistochemical detection of tumor markers in breast cancer tissue using laser ablation inductively coupled plasma mass spectrometry. Anal Chem. 2011;83:8177–83. https://doi.org/10.1021/ac2016823.
16. Paul B, Hare DJ, Bishop DP, Paton C, Nguyen VT, Cole N, et al. Visualising mouse neuroanatomy and function by metal distribution using laser ablation-inductively coupled plasma-mass spectrometry imaging. Chem Sci. 2015;6:5383–93. https://doi.org/10.1039/C5SC02231B.
17. Waentig L, Techritz S, Jakubowski N, Roos PH. A multi-parametric microarray for protein profiling: simultaneous analysis of 8 different cytochromes via differentially element tagged antibodies and laser ablation ICP-MS. Analyst. 2013;138:6309–15. https://doi.org/10.1039/c3an00468f.
18. Hare D, Austin C, Doble P. Quantification strategies for elemental imaging of biological samples using laser ablation-inductively coupled plasma-mass spectrometry. Analyst. 2012;137:1527–37. https://doi.org/10.1039/c2an15792f.
19. Vizoso FJ, González LO, Corte MD, Rodríguez JC, Vázquez J, Lamelas ML, et al. Study of matrix metalloproteinases and their inhibitors in breast cancer. Br J Cancer. 2007;96:903–11. https://doi.org/10.1038/sj.bjc.6603666.

20. de Vega RG, Sanchez MLF, Eiro N, Vizoso FJ, Sperling M, Karst U, et al. Multimodal laser ablation/desorption imaging analysis of Zn and MMP-11 in breast tissues. Anal Bioanal Chem. 2018;410:913–22. https://doi.org/10.1007/s00216-017-0537-x.
21. Hare DJ, George JL, Bray L, Volitakis I, Vais A, Ryan TM, et al. The effect of paraformaldehyde fixation and sucrose cryoprotFection on metal concentration in murine neurological tissue. J Anal At Spectrom. 2014;29:565–70. https://doi.org/10.1039/C3JA50281C.
22. Cruz-Alonso M, Fernandez B, Álvarez L, González-Iglesias H, Traub H, Jakubowski N, et al. Bioimaging of metallothioneins in ocular tissue sections by laser ablation-ICP-MS using bioconjugated gold nanoclusters as specific tags. Microchim Acta. 2018;185:64. https://doi.org/10.1007/s00604-017-2597-1.